IOPscience iopscience.iop.org

Home Search Collections Journals About Contact us My IOPscience

Correlation between crystal structure and photoluminescence for epitaxial ZnO on Si (1 1 1) using a γ-Al_2O_3 buffer layer

This content has been downloaded from IOPscience. Please scroll down to see the full text.

2008 J. Phys. D: Appl. Phys. 41 065105

(http://iopscience.iop.org/0022-3727/41/6/065105)

View the table of contents for this issue, or go to the journal homepage for more

Download details:

IP Address: 140.113.38.11
This content was downloaded on 25/04/2014 at 17:00

Please note that terms and conditions apply.

J. Phys. D: Appl. Phys. **41** (2008) 065105 (5pp) doi:10.1088/0022-3727/41/6/065105

Correlation between crystal structure and photoluminescence for epitaxial ZnO on Si (1 1 1) using a γ-Al_2O_3 buffer layer

W-R Liu[1], Y-H Li[1], W F Hsieh[1,5], C-H Hsu[1,2,5], W C Lee[3], M Hong[3] and J Kwo[4]

[1] Department of Photonics and Institute of Electro-Optical Engineering, National Chiao Tung University, Hsinchu 30010, Taiwan
[2] Research Division, National Synchrotron Radiation Research Center, Hsinchu 30076, Taiwan
[3] Department of Materials Science and Engineering, National Tsing Hua University, Hsinchu 30013, Taiwan
[4] Department of Physics, National Tsing Hua University, Hsinchu 30013, Taiwan

E-mail: wfhsieh@mail.nctu.edu.tw and chsu@nsrrc.org.tw

Received 23 November 2007, in final form 5 February 2008
Published 29 February 2008
Online at stacks.iop.org/JPhysD/41/065105

Abstract
High-quality ZnO epitaxial films were grown by pulsed-laser deposition on Si (1 1 1) substrates with a thin γ-Al_2O_3 buffer layer. The epitaxial γ-Al_2O_3 buffer layer consists of two (1 1 1) oriented domains rotated 60° from each other against the surface normal, which yields the in-plane epitaxial relationship $(1\,0\,0)_{ZnO}||\{2\,2\,\bar{4}\}_{\gamma\text{-}Al_2O_3}$ or $\{4\,\bar{2}\,\bar{2}\}_{\gamma\text{-}Al_2O_3}||\{2\,2\,\bar{4}\}_{Si}$. The crystalline quality and optical properties of ZnO epi-layers were studied by x-ray diffraction and photoluminescence measurements. A clear correlation between ZnO deep-level emission (DLE) to near-band edge (NBE) emission intensity ratio and the width of the ϕ-scan across off-normal reflection was observed. The NBE linewidth also exhibits strong dependence on the width of the ZnO (0 0 2) rocking curve. These observations indicate the NBE and DLE emissions are mainly affected by the edge and screw type dislocations, respectively.

1. Introduction

Wurtzite ZnO is a II–VI semiconductor with a wide direct band gap of 3.37 eV. It has potential application for UV/blue light-emitting diodes (LED) and lasers at high temperatures as a result of the large exciton binding energy of 60 meV [1]. Recently, much attention has been paid to heteroepitaxially grown ZnO on Si substrates because of the unique possibility of integrating well-established Si electronics with ZnO-based optoelectronic devices. Unfortunately, direct growth of epitaxial ZnO films on Si is an extremely difficult task due to the formation of an amorphous SiO_2 layer at the ZnO/Si interface [2, 3] that usually results in polycrystalline films with preferred orientation [4]. Although significant efforts have been made to use nonoxide materials, such as ZnS [2], Si_3N_4 [3], Zn/MgO [5] and Mg/MgO [6], as buffer layers, the growth of high-quality ZnO epi-films on Si is still regarded as an arduous challenge.

The other issue for the growth of high-quality ZnO epi-films is the existence of high-density threading dislocations (TDs) originating from the large difference in the lattice mismatch (−15.4%) and the thermal expansion coefficient (56%) between ZnO (thermal expansion coefficient $\alpha \sim 5 \times 10^{-6}\,K^{-1}$ [7], lattice parameters $a = 3.24$ Å, $c = 5.20$ Å) and underneath the Si substrate ($\alpha = 3.6 \times 10^{-6}\,K^{-1}$ [8], $a = 5.431$ Å). The point defects captured by TDs stress field act as traps and recombination sites forming deep electronic states inside the band gap [9, 10]. They can lead to electron scattering [11], significantly affect the optical performance and electron mobility [10, 12] and adversely demote the device efficiency. In this paper, we report the growth of high-quality epitaxial ZnO films using pulsed-laser deposition (PLD) on Si (1 1 1) substrates with a ∼15.3 nm thick γ-Al_2O_3 film as the buffer layer. The good crystal structure of thin ZnO films was confirmed by x-ray diffraction (XRD) and transmission electron microscopy (TEM). Their optical characteristics were studied using photoluminescence (PL) and correlated with its structural properties.

[5] Author to whom any correspondence should be addressed.

 © 2008 IOP Publishing Ltd Printed in the UK

2. Experiment

The cubic γ-Al_2O_3 layer, with lattice constant $a = 7.91$ Å and thermal expansion coefficient $\alpha = 8.2 \times 10^{-6}\,K^{-1}$ [13], was deposited on Si (1 1 1) at 720 °C using electron beam evaporation from a high-purity single crystal sapphire source in a multi-chamber molecular beam epitaxy (MBE) system. The details of γ-Al_2O_3 growth were described elsewhere [14]. ZnO was subsequently grown by PLD [15]. The beam out of a KrF excimer laser ($\lambda = 248$ nm) was focused to produce an energy density ~5–7 J cm^{-2} at a repetition rate of 10 Hz on a commercial hot-pressed stoichiometric ZnO (5 N) target. ZnO was deposited at a substrate temperature ranging from 200 to 500 °C without introducing oxygen gas flow during growth and the growth rate was ~0.40 Å s^{-1}. Two batches of samples grown on two composite substrates, which were prepared under the same deposition conditions, were studied. The first batch has a thickness of $0.29 \pm 0.04\,\mu$m and the thickness of the second batch is $0.20 \pm 0.02\,\mu$m. XRD measurements were performed with a four-circle diffractometer at the wiggler beamline BL17A of National Synchrotron Radiation Research Center, Taiwan, with incident wavelength 1.3344 Å. Two pairs of slits, located between the sample and a NaI scintillation detector, were employed and yielded a typical resolution of 4×10^{-3} Å^{-1}. Cross sectional TEM images were taken using a field-emission-gun type TEM (Philips TECNAI-20). The PL measurement was carried out using a He–Cd laser of wavelength 325 nm as pumping source. The light emission was dispersed by a Triax-320 spectrometer and detected by an UV-sensitive photomultiplier tube.

3. Results and discussion

A radial scan along the surface normal (θ–2θ scan) of the ZnO layer grown at 300 °C is illustrated in figure 1, where the abscissa $q_z = 4\pi \sin(\theta)/\lambda$ denotes the momentum transfer along the surface normal and λ is the incident x-ray wavelength. Only ZnO (0 0 2), γ-Al_2O_3 (1 1 1) and (2 2 2) and Si (1 1 1) reflections were observed, elucidating a crystalline orientation of $(0\,0\,2)_{ZnO}||(1\,1\,1)_{\gamma\text{-}Al_2O_3}||(1\,1\,1)_{Si}$ along the surface normal. The pronounced thickness fringe observed near the γ-Al_2O_3 (2 2 2) reflection indicates the sharpness of the γ-Al_2O_3 interfaces; the fringe period yields a layer thickness of ~15.3 nm. From the full width at half maximum (FWHM) of the γ-Al_2O_3 (2 2 2) reflection, we derived the vertical coherence length of the buffer layer, using the Scherrer's equation, to be ~15 nm, which is close to the layer thickness. This implies that the structural coherence of the buffer layer is maintained over almost the entire layer thickness.

Azimuthal cone scans (ϕ-scans) across the off-normal ZnO {1 0 1}, γ-Al_2O_3 {4 4 0} and Si {2 2 0} reflections, as illustrated in figure 2, were measured to examine the in-plane epitaxial relationship. Six evenly spaced ZnO diffracted peaks verified that the hexagonal ZnO film was epitaxially grown on the γ-Al_2O_3/Si (1 1 1) composite substrate. Furthermore, two sets of peaks with 3-fold symmetry were observed in the γ-Al_2O_3 {4 4 0} ϕ-scan, revealing the cube-on-cube growth

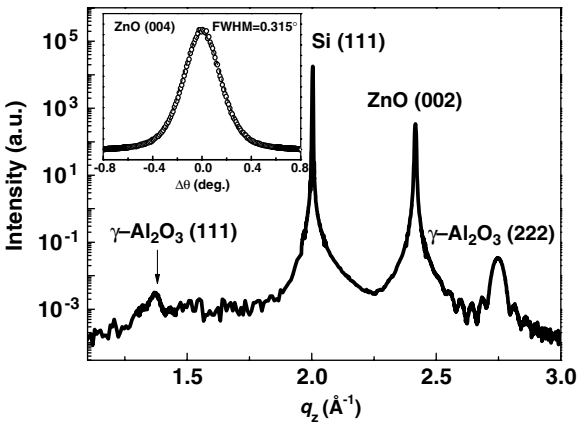

Figure 1. XRD radical scan along the surface normal of a 0.3 μm thick ZnO layer grown on the γ-Al_2O_3/Si (1 1 1) composite substrate. The inset illustrates a θ-rocking curve of ZnO (0 0 4) reflection.

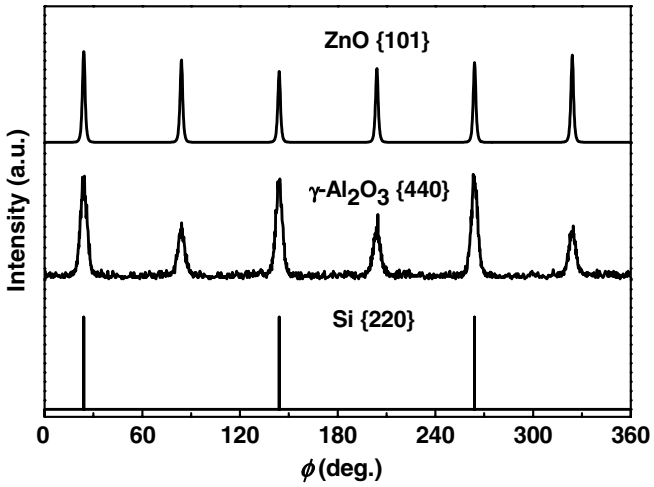

Figure 2. The profiles of ϕ-scans across ZnO {1 0 1}, γ-Al_2O_3{4 4 0} and Si {2 2 0} reflections

of γ-Al_2O_3 on Si and the coexistence of two in-plane rotated variants. The dominant one has the same angular position as that of the Si {2 2 0}, A-type (1 1 1) orientated domain, and the minor one has its in-plane orientation rotated 60° from that of Si substrate, B-type domain [16]. These results suggest that the in-plane epitaxial relationship of this hetero-epitaxial system follows $(1\,0\,0)_{ZnO}||\{2\,2\,\bar{4}\}_{\gamma\text{-}Al_2O_3}$ or $\{4\,\bar{2}\,\bar{2}\}_{\gamma\text{-}Al_2O_3}||\{2\,2\,\bar{4}\}_{Si}$. In this geometry, the two-dimensional hexagonal unit cell of the γ-Al_2O_3 (1 1 1) plane is aligned with that of the ZnO basal plane with its lattice constant equal to $\sqrt{2} \cdot a(\gamma\text{-}Al_2O_3) = 11.186$ Å, about 3.45 times larger than that of ZnO.

Within the employed growth temperature range, all the samples exhibit the same structural characteristics with a small variation of less than 0.2% in ZnO lattice parameters. The lattice parameters of the ZnO layer grown at 300 °C were measured to be $a = 3.2528$ Å and $c = 5.1937$ Å. As compared with the bulk values, $a = 3.2438$ Å and $c = 5.2036$ Å determined from a ZnO wafer, we found that all the ZnO epitaxial films experienced a tensile strain (~0.28%) in the lateral direction and were compressively stressed (~0.19%) along the surface normal. The mosaicity of the film against

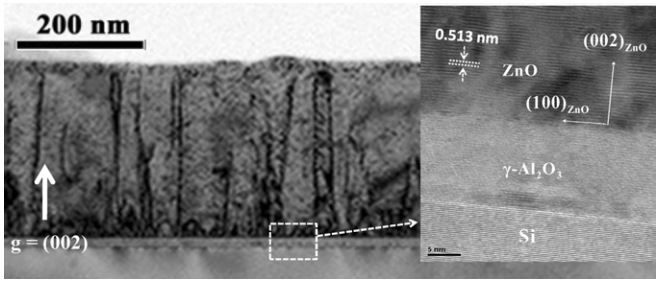

Figure 3. Two-beam bright-field cross-sectional TEM micrographs of the ZnO film with $g = (0\,0\,2)_{ZnO}$. The inset is the cross-sectional HR-TEM micrograph taken near the interfacial region with the $[1\,0\,\bar{1}]_{Si}$ projection.

the sample normal, i.e. the tilt angle, was characterized by measuring the θ-rocking curve of the ZnO (0 0 2) and the (0 0 4) diffraction peaks and fitting the Williamson and Hall plot. The small values of FWHM, 0.32°–0.61° with the minimum obtained at 300 °C, as shown in the inset of figure 1, manifest the good crystalline quality of ZnO epi-layers even for films as thin as 0.3 μm. This value is comparable to that of ZnO epi-layers grown on nonoxide buffer layers, such as ZnS ($\Delta\theta = 0.25°$, film thickness = 0.35 μm) [2], Al (0.35°, 1 μm) [17] and 3C-SiC (1.11°, 0.25 μm) [18]. The twist of the ZnO lattice against the surface normal was determined from the peak width of azimuthal scans of in-plane and off-normal reflections. The obtained twist angle falls between 1.4° and 4.3° depending on the growth conditions. From the structure of ZnO grown on different batches of buffer layer, we found that the quality of ZnO epi-films is sensitive to the structural perfection of the γ-Al_2O_3 buffer layer. However, the lateral domain size and tilt/twist angles of the ZnO layers are always better than the underneath buffer layer and exhibit progressive improvement with increasing film thickness. It is worth noting that for a given film thickness an increase of $\Delta\theta$ is always accompanied by a decrease in $\Delta\phi$ and the ZnO epi-layers grown on γ-Al_2O_3 buffer at 300 °C always have the smallest tilt angle but the largest twist angle. This is different from ZnO grown on other substrates, such as *c*-plane sapphire, where tilt and twist angles always exhibit the same trend of increase/decrease with growth conditions [15]. This negative correlation between the tilt and twist angles allows us to separate their influence on the optical properties of the ZnO epi-layers, which will be discussed later.

Figure 3 shows the cross-sectional TEM bright-field image with $\boldsymbol{g} = (0\,0\,2)_{ZnO}$ under a two-beam contrast condition. The major defect structure in the ZnO layer is TDs seen as dark lines stemming from the ZnO/γ-Al_2O_3 interface with their dislocation lines primarily along the [0 0 1] direction. The average TD density is about 3×10^{10} cm^{-2}, as determined from the TEM image and XRD line width analyses, independently. Employing the two-beam condition with different $\boldsymbol{g}$ vectors (0 0 2), (1 1 0) and (1 1 2) selected, we also found that TDs with edge component are predominant, with its density an order of magnitude higher than that of TDs with screw component. The high magnification TEM image taken at the interfacial region with $[1\,0\,\bar{1}]_{Si}$ projection, shown in the inset of figure 3, reveals unequivocal interfaces of ZnO/γ-Al_2O_3 and γ-Al_2O_3/Si. No

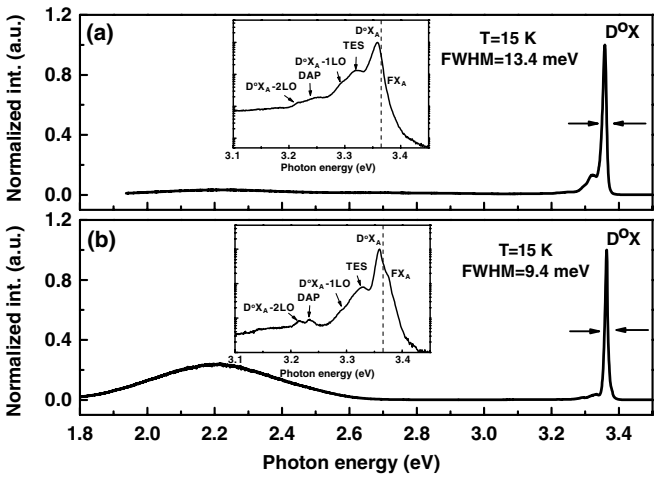

Figure 4. Typically PL spectra measured at 15 K for ZnO epi-layers deposited on γ-Al_2O_3/Si (1 1 1) at 200 °C (*a*) and 300 °C (*b*). The insets in (*a*) and (*b*) are the extended spectra of NBE emission. The dashed lines mark the D^oX peak position of bulk ZnO.

intermediate layer was observed in either interface. These results demonstrate that the growth of high-quality ZnO epi-films on Si using an oxide buffer layer is possible and a γ-Al_2O_3 layer serves well as a template for subsequent ZnO growth.

The optical properties of ZnO/γ-Al_2O_3/Si epi-layers were explored by using low temperature (LT) PL measurements at 15 K. The PL spectra of ZnO films grown at 200 °C and 300 °C are displayed in figures 4(*a*) and (*b*), respectively. Regardless of the growth temperature, the main features in PL spectra are common for all samples and can be divided into two categories: the near-band edge (NBE) emission and deep-level emission (DLE). The assignments of NBE peaks are also shown in the insets of figures 4(*a*) and (*b*). The peak at 3.375 eV was assigned as the free A-exciton (FX_A) line; the binding energy of the corresponding A-exciton was obtained to be 58.875 meV by fitting the temperature-dependent PL data using the Arrhenius expression. The dominant peak at ~3.359 eV and ~3.364 eV in the NBE region were assigned to the recombination of excitons bound to neutral donor (D°X) [19] and their FWHM are 13.4 and 9.4 meV in (*a*) and (*b*), respectively. The D°X emission accompanied with single phonon (D°X–1LO) and dual phonon (D°X–2LO) replica appear at 3.288 and 3.215 eV. The peak at ~3.23 eV is attributed to the donor–acceptor pair (DAP) transition. Another strong line at 3.328 eV originates from the transition involving radiative recombination of an exciton bound to a neutral donor (D°X) and leaving the donor in the excited state. This process is also known as the two-electron satellite (TES). We made such an assignment based on the ratio of donor binding energy to exciton binding energy ~0.35, as reported by Teke *et al* [19]. Similarly to the E_2-high mode in the Raman spectra of ZnO thin films [20], the position of the D°X is sensitive to the strain state of the films. The observed red shift of D^oX energy relative to that of ZnO bulk wafer (3.365 eV), marked by the dashed lines in the insets of figure 4, is consistent with the biaxial tensile strain determined by XRD measurements. The broad DLE peak centring at ~2.196 eV has its intensity ratio to the NBE feature (I_{DLE}/I_{NBE}) being

0.032 and 0.24 for 200 and 300 °C grown samples. The DLE emission is attributed to the transitions involving point defects such as O vacancies, Zn interstitials as well as other surface defects and its strength is positively correlated with the defect density [21,22]. Post-growth annealing in O_2 atmosphere did lead to a significant reduction of DLE emission, indicating that O vacancies are a major source of DLE emission. The brighter intensity and narrower line width of NBE and the low (I_{DLE}/I_{NBE}) intensity ratio are considered as signatures of better optical properties. Comparing the PL spectra of ZnO grown at 200 and 300 °C, we found that the optical performance of ZnO grown at 300 °C was better in the NBE but worse in the DLE region. We also observed that the tilt/twist angle of the sample grown at 300 °C is smaller/larger than that grown at 200 °C. Previous studies pointed out that the tilt angle alone, which is coupled with the screw type TDs, is not sufficient to describe the crystalline quality of the ZnO films [15,23]. Twist angle, which is a measure of edge type TD density, should be taken into consideration to account for the optical properties. The different trend of increase/decrease of the tilt and twist angles with growth conditions observed in this case allows us to independently examine the influence of edge and screw TDs.

The (I_{DLE}/I_{NBE}) ratio versus $\Delta\phi_{(1\,0\,1)}$, the FWHM of the azimuthal scan across ZnO off-normal (1 0 1) reflection, and the FWHM of NBE versus $\Delta\theta_{(0\,0\,2)}$, the FWHM of the rocking curve of the (0 0 2) specular reflection, are illustrated in figures 5(*a*) and (*b*), respectively. Here $\Delta\phi_{(1\,0\,1)}/\Delta\theta_{(0\,0\,2)}$ bears the same physical meaning as the twist/tilt angle and can be considered as a measure of the density of edge/screw TDs. In both figures, (I_{DLE}/I_{NBE}) ratio and FWHM of NBE exhibit monotonic increases with $\Delta\phi_{(1\,0\,1)}$ and $\Delta\theta_{(0\,0\,2)}$, respectively. In contrast, the distribution of the (I_{DLE}/I_{NBE}) ratio scatters randomly with $\Delta\theta_{(0\,0\,2)}$ and the line width of NBE did not show a clear correlation with $\Delta\phi_{(1\,0\,1)}$, either. Evidently, the NBE emission is predominantly governed by the screw component of the TDs and the edge TDs play the key role in affecting the DLE intensity. Our observations support the arguments that screw TDs can act as nonradiative centres in reducing the NBE emission intensity, and the existence of edge TDs leads to aggregation of point defects due to stress field near the dislocation core resulting in the enhancement of DLE intensity [10,24]. Consequently, reducing TDs density of both types in the growth of ZnO epitaxial film is still an important issue in the applications to photonic devices.

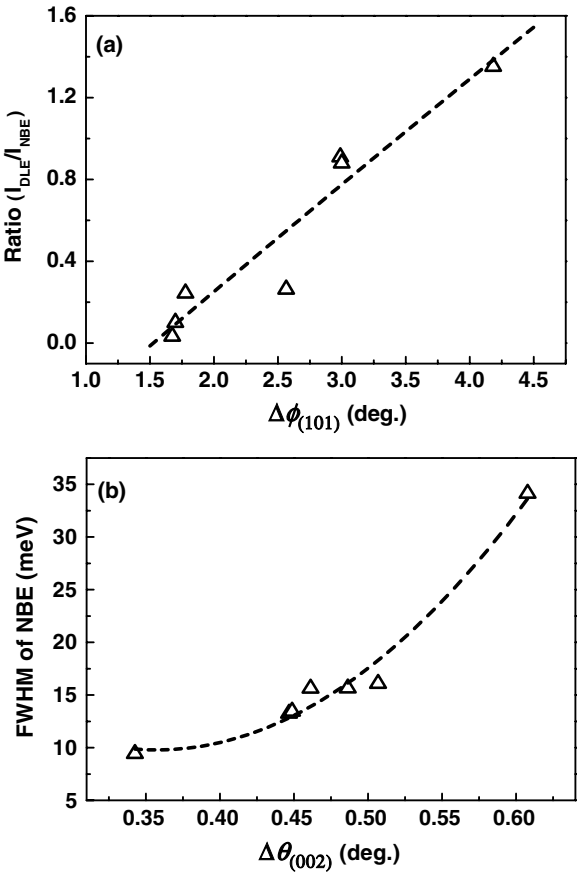

Figure 5. The dependence of (I_{DLE}/I_{NBE}) ratio on $\Delta\phi$ of ZnO (1 0 1) diffracted peak (*a*). The dependence of NBE width $\Delta\theta$ of ZnO (0 0 2) diffracted peak (*b*). The dash curves are plotted to guide the eyes.

4. Summary

In this work, we have successfully grown high-quality ZnO epitaxial films by PLD on Si (1 1 1) substrates with a nano-thick γ-Al_2O_3 buffer layer. There exist two (1 1 1)-oriented γ-Al_2O_3 domains rotated 60° from each other relative to the surface normal. The in-plane epitaxial relationship between the wurtzite ZnO, cubic γ-Al_2O_3 and cubic Si follows $(1\,0\,0)_{ZnO}||\{2\,2\,\bar{4}\}_{\gamma\text{-}Al_2O_3}$ or $\{4\,\bar{2}\,\bar{2}\}_{\gamma\text{-}Al_2O_3}||\{2\,2\,\bar{4}\}_{Si}$, as determined by XRD and TEM. The connection between the defect characterisitcs and the optical properties of the ZnO layer was established by correlating XRD and LT-PL results. Our results indicate that the (I_{DLE}/I_{NBE}) ratio is dominantly affected by edge TDs and the line width of NBE emission is mainly related to screw TDs.

Acknowledgments

This work is partly supported by the National Science Council of Taiwan under grants NSC-96-2119-M-213-003 and NSC-96-2628-M-009-001-MY3.

References

[1] Tsukazaki A *et al* 2005 *Nature Mater.* **4** 42
[2] Yoo Y Z, Sekiguchi T, Chikyow T, Kawasaki M, Onuma T, Chichibu S F, Song J H and Koinuma H 2004 *Appl. Phys. Lett* **84** 502
[3] Lin C C, Chen S Y, Cheng S Y and Lee H Y 2004 *Appl. Phys. Lett.* **84** 5040
[4] Cheng H M, Hsu H C, Yang S, Wu C Y, Lee Y C, Lin L J and Hsieh W F 2005 *Nanotechnology* **16** 2882
[5] Fujita M, Kawamoto N, Sasajima M and Horikoshi Y 2004 *J. Vac. Sci. Technol.* B **22** 1484
[6] Wang X N *et al* 2007 *Appl. Phys. Lett.* **90** 151912
[7] Vispute R D *et al* 1998 *Appl. Phys. Lett.* **73** 348
[8] Nahhas A, Kim H K and Blachere J 2001 *Appl. Phys. Lett.* **78** 1511
[9] Oyama Y, Nishizawa J, Kimura T and Tanno T 2006 *Phys. Rev.* B **74** 235210

[10] Bangert U, Harvey A J, Jones R, Fall C J, Blumenau A, Briddon R, Schreck M and Hörmann F 2004 *New J. Phys.* **6** 184
[11] Ng H M, Doppalapudi D, Moustakas T D, Weimann N G and Eastman L F 1998 *Appl. Phys. Lett.* **73** 821
[12] Shi J Y, Yu L P, Wang Y Z, Zhang G Y and Zhang H 2002 *Appl. Phys. Lett.* **80** 2293
[13] Kollenberg W and Margalit J 1992 *J. Mater. Sci. Lett.* **11** 991
[14] Wu S Y, Hong M, Kortan A R, Kwo J, Mannaerts J P, Lee W C and Huang Y L 2005 *Appl. Phys. Lett.* **87** 091908
[15] Liu W R, Hsieh W F, Hsu C H, Liang K S and Chien F S S 2007 *J. Appl. Cryst.* **40** 924
[16] Tung R T and Batstone J L 1988 *Appl. Phys. Lett.* **52** 1611
[17] Chen Y, Jiang F, Wang L, Zheng C, Dai Y, Pu Y and Fang W 2005 *J. Cryst. Growth* **275** 486
[18] Zhu J, Lin B, Sun X, Yao R, Shi C and Fu Z 2005 *Thin Solid Films* **478** 218
[19] Teke A, Özgür Ü, Dogan S, Gu X, Morkoç H, Nemeth B, Nause J and Everitt H O 2004 *Phys. Rev.* B **70** 195207
[20] Shen W J, Wang J, Wang Q Y, Duan Y and Zeng Y P 2006 *J. Phys. D: Appl. Phys.* **39** 269
[21] Chen Y F, Bagnall D M, Koh H J, Park K T, Hiraga K, Zhu Z and Yao T 1998 *J. Appl. Phys.* **84** 3912
[22] Onuma T, Chichibu S F, Uedono A, Yoo Y Z, Chikyow T, Sota T, Kawasaki M and Koinuma H 2004 *Appl. Phys. Lett.* **85** 5586
[23] Zhang B P, Segawa Y, Wakatsuki K, Kashiwaba Y and Haga K 2001 *Appl. Phys. Lett.* **79** 3953
[24] You J H and Johnson H T 2007 *J. Appl. Phys.* **101** 023516